

# Chemical transport in mixed conductors: Application to the model materials SrTiO<sub>3</sub> and ZrO<sub>2</sub>

J. Maier\* and W. Münch

Max-Planck-Institut für Festkörperforschung Heisenbergstraße 1, 70569 Stuttgart, Germany

The effect of internal ionisation equilibria of dopants on chemical diffusion is discussed in detail and applied to the cases of SrTiO<sub>3</sub> and yttria-stabilised ZrO<sub>2</sub>. In particular, the sensitive dependence of the diffusion coefficient on the position of the impurity level is highlighted. Two major cases are worth distinguishing: One in which the redox-active dopant is in a minority and a second one in which it plays a major role in the equation of electroneutrality. In contrast to the equilibrium case, the concentration of redox-active dopants is of pronounced importance for chemical diffusion in both cases. The significance for applications is also discussed.

## 1. Introduction

If there is a perturbation in the equilibrium composition, chemical diffusion is the relevant process which drives the system back to equilibrium. The relevant transport coefficient is the chemical diffusion coefficient,  $\tilde{D}$ . Table 1 gives an overview of some typical values and the related equilibrium times for one-dimensional diffusion in a 1 mm thick pellet.

Values of  $\tilde{D}$  of the order of  $10^{-3} \text{ cm}^2 \text{ s}^{-1}$  are about the upper limit, *i.e.* unless the dimensions are not reduced, equilibration times cannot be much longer than a few seconds in the linear response regime. Usually, diffusion coefficients are lower by many orders of magnitude. For values of  $10^{-6} \text{ cm}^2 \text{ s}^{-1}$ , equilibration times are of the order of an hour, values of  $10^{-10} \text{ cm}^2 \text{ s}^{-1}$  demand some years to reach equilibrium. Values of the order of  $10^{-20}$  exclude the possibility of spatial equilibration at all, since the corresponding waiting times exceed the age of the Earth. In addition, these times are lower limits since diffusion occurs in series with boundary processes. Low  $\tilde{D}$  values are not only necessary for the structuring of natural and man-made products, they are also a prerequisite for the functioning of devices. Doping metastability in silicon-based devices, morphological metastability of quantum wells and living organisms, and metastability of human skin and nucleobase sequences are striking examples in this context. In the field of electroceramics an appropriate example would be a surface conductivity sensor, *e.g.* a low-temperature oxygen sensor that employs the boundary resistance changes of SnO<sub>2</sub> works well and drift-free only if the oxygen bulk equilibration is negligible. On the other hand, devices such as bulk conductivity sensors or chemical filters require rapid oxygen diffusion.

**Table 1** Equilibration times<sup>a</sup> for one-dimensional diffusion in a 1 mm pellet

$\tilde{D}/\text{cm}^2 \text{ s}^{-1}$	$\tau_{\text{eq}}/\text{s}$ ( $L = 1 \text{ mm}$ )
$10^{-20}$	$5 \times 10^{17}$ (> Earth's age)
$10^{-10}$	$5 \times 10^7$ (ca. 1–5 years)
$10^{-8}$	$5 \times 10^5$ (ca. 1 week)
$10^{-6}$	$5 \times 10^3$ (ca. 1 h)
$10^{-5}$	$5 \times 10^2$ (ca. 10 min)
$10^{-4}$	50 (ca. 1 min)
$10^{-3}$	5
$10^{-2}$	0.5 (fluid phases)

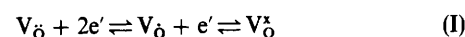
<sup>a</sup> More precisely,  $\tau_{\text{eq}}$  corresponds to the time taken until the concentration change resulting from a sudden change in  $P_{\text{O}_2}$  (on both symmetrical sides of the pellet) is 99% of the equilibrium change [ $\tau_{\text{eq}} \equiv L^2/(2\tilde{D})$ ].

## 2. General remarks on chemical diffusion in crystalline solids

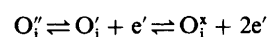
For dilute crystalline bulk systems in which no internal reactions are important, the chemical diffusion process is very clear and well understood.<sup>1</sup> Mass transport is determined by the fluxes of at least two carriers coupled in such a way that local electroneutrality is maintained. If we consider (in order to be more specific) the oxygen flux in a binary or a quasi-binary oxide  $\text{M}^{2+}\text{O}^{2-}$ , the oxygen flux, *i.e.* the redox flux, is composed of counter-fluxes of  $\text{O}^{2-}$  ( $j_{\text{O}^{2-}}$ ) and  $\text{e}^-$  ( $j_{\text{e}^-} = -2j_{\text{O}^{2-}}$ ). If the oxygen defect is a vacancy ( $j_{\text{O}^{2-}} = -j_{\text{V}_\text{O}}$ ) and the electronic defects are conduction electrons ( $j_{\text{e}^-} = j_{\text{e}^+}$ ) it follows that  $2j_{\text{V}_\text{O}} = j_{\text{e}^+}$ . For dilute defects this results in a Fick's law type behaviour with a diffusion coefficient ( $\tilde{D}$ ) that is in between the diffusivities of  $\text{V}_\text{O}$  and  $\text{e}^+$ . We obtain<sup>2</sup>

$$\tilde{D} = \frac{\sigma_{\text{e}^+}}{\sigma} D_{\text{V}_\text{O}} + \frac{\sigma_{\text{V}_\text{O}}}{\sigma} D_{\text{e}^+} = \frac{D_{\text{e}^+} D_{\text{V}_\text{O}} F^2}{\sigma RT} (z_{\text{e}^+}^2 c_{\text{e}^+} + z_{\text{V}_\text{O}}^2 c_{\text{V}_\text{O}}) \quad (1)$$

which reduces for  $c_{\text{e}^+} \gg c_{\text{V}_\text{O}}$  or  $c_{\text{V}_\text{O}} \gg c_{\text{e}^+}$  to  $\sigma_{\text{e}^+}/\sigma D_{\text{V}_\text{O}}$  or to  $\sigma_{\text{V}_\text{O}}/\sigma D_{\text{e}^+}$ , respectively (since the ratio of the charge numbers,  $z_i$ , is not far from 1). Note that the  $D$ s refer to the defects and not to the ions or electrons as such. The situation changes if internal sources and sinks have to be considered even if the reactions coupled to the diffusion process are in local equilibrium.<sup>3</sup> As shown<sup>3,4</sup> by one of the authors, in the general case that vacancies and interstitials are present in different valence states, *i.e.* reactions such as



and



couple to the transport, the result is more complicated and reads for dilute defects as:

$$\tilde{D} = \frac{RT}{4F^2} \left[ 2(\sigma_{\text{O}_\text{i}} + \sigma_{\text{V}_\text{O}}) + \frac{4F^2}{RT} (D_{\text{V}_\text{O}} c_{\text{V}_\text{O}} + D_{\text{O}_\text{i}^+} c_{\text{O}_\text{i}^+}) + \frac{(\sigma_{\text{O}_\text{i}} + \sigma_{\text{V}_\text{O}} + 2\sigma_{\text{O}_\text{i}'} + 2\sigma_{\text{V}_\text{O}'})(\sigma_{\text{e}^+} + \sigma_{\text{H}} - \sigma_{\text{V}_\text{O}} - \sigma_{\text{O}_\text{i}})}{\sigma} \right] \times \left( \frac{\chi_{\text{V}_\text{O}}}{c_{\text{V}_\text{O}}} + 4 \frac{\chi_{\text{e}^+}}{c_{\text{e}^+}} \right) \quad (2)$$

with  $\chi_{\text{V}_\text{O}} \equiv -\delta c_{\text{V}_\text{O}}/\delta c_{\text{O}_2}$ ,  $\chi_{\text{e}^+} \equiv -\frac{1}{2} \delta c_{\text{e}^+}/\delta c_{\text{O}_2}$ . Of course, the  $(\chi/c)$

factors could be equivalently expressed in terms of other defects. Eqn. (2) also includes electronic holes ( $h^\bullet$ ) as carriers.

The case is simpler if the native defects are fully ionised, but redox-active impurities are present which are immobile but change their valence states. To be specific with respect to the examples under study here, we consider acceptor dopants, holes and oxygen vacancies to be the relevant charge carriers. The valence change of A is expressed by the ionisation reaction



In the following text, we sometimes denote for brevity  $A^{(n+1)'}$  and  $A^{n'}$  as red and ox, respectively. Owing to mass conservation the sum of  $[ox]$  and  $[red]$  is constant which we henceforth call  $m$ , i.e.  $[A^{n'}] + [A^{(n+1)'}] = m$ . Then, instead of eqn. (1) we obtain

$$\begin{aligned} \tilde{D} &= \chi_{h^\bullet} \frac{\sigma_{V_\delta}}{\sigma} D_{h^\bullet} + \frac{\sigma_{h^\bullet}}{\sigma} D_{V_\delta} \\ &= \frac{D_{h^\bullet} D_{V_\delta} F^2}{\sigma R T} (z_{V_\delta}^2 c_{V_\delta} + \chi_{h^\bullet} z_{h^\bullet}^2 c_{h^\bullet}) \end{aligned} \quad (3)$$

which simplifies to  $\tilde{D} = \chi_{h^\bullet} \sigma_{V_\delta} / \sigma D_{h^\bullet}$  for  $c_{V_\delta} \chi_{h^\bullet} \gg c_{h^\bullet} / 4$ . In eqn. (3), in which  $\chi_{h^\bullet}$  denotes the differential change in the number of free holes ( $h^\bullet$ ) with respect to the total number, i.e. the number of free ( $h^\bullet$ ) and trapped holes (ox) [according to reaction (II)] which can be calculated from the local equilibrium of reaction (II), it has to be kept in mind that  $\chi$  cannot be obtained from the incorporation reaction treating  $P_{O_2}$  as a constant. Rather, the derivative has to be calculated at constant temperature,  $T$ , and dopant content,  $m$ ; the local oxygen partial pressure ( $P_{O_2}$ ), however, is a variable; otherwise no stoichiometric changes would occur. The formal reason is that  $\chi$  varies according to  $d\mu_0/dc_0$ ,<sup>3</sup> which automatically includes variations of  $P_{O_2}$ .

To be more general, we include the possibility of having simultaneously several internal redox reactions of the form



i.e. we are allowing for the presence of different redox-active species. Considering  $h^\bullet$  and  $V_\delta$  as the native carriers, electroneutrality reads as

$$\begin{aligned} 2[V_\delta] + [h^\bullet] &= \sum_i (n_i + 1) [A_i^{(n_i+1)'}] + \sum_i n_i [A_i^{n_i'}] \\ &= \sum_i (n_i + 1) m_i - \sum_i [A_i^{n_i'}] \end{aligned} \quad (4)$$

As the individual total dopant concentrations ( $m_i \equiv [A_i^{n_i'}] + [A_i^{(n_i+1)'}]$ ) can be considered to be constant owing to their immobility, we obtain for the differential form of the electroneutrality equation (change during a chemical diffusion experiment)

$$2\delta[V_\delta] + \delta[h^\bullet] = -\sum_i \delta[A_i^{n_i'}] \quad (5)$$

or

$$\begin{aligned} +2\delta[O^*] &\equiv -2\delta[V_\delta] \\ &= \delta[h^\bullet] + \sum_i \delta[A_i^{n_i'}] \approx -\delta[e^*] \approx \delta[h^*] \end{aligned} \quad (6)$$

In eqn. (6) the conservative ensembles  $[O^*]$  and  $[e^*]$  (or  $[h^*]$ ) have been introduced in a defining manner.<sup>3,4</sup> Taking account of the definition  $\chi_{h^\bullet} = \delta[h^\bullet]/\delta[h^*]$  and the mass action constants for reaction (III), viz.

$$K_i = \frac{[A_i^{(n_i+1)'}][h^\bullet]}{[A_i^{n_i'}]} = \frac{(m - [A_i^{n_i'}])[h^\bullet]}{[A_i^{n_i'}]} \quad (7)$$

we infer

$$\chi_{h^\bullet}^{-1} = 1 + \sum_i \frac{\delta[A_i^{n_i'}]}{\delta[h^\bullet]} = 1 + \sum_i \frac{m_i K_i}{(K_i + [h^\bullet])^2} \quad (8)$$

For more details see ref. 5 and 6. The term  $[h^*]$  can be calculated as a function of  $P_{O_2}$ ,  $T$ ,  $m_i$  from the defect chemistry assuming local equilibrium.

### 3. Application to $\text{SrTiO}_3$ and $\text{ZrO}_2(\text{Y}_2\text{O}_3)$

Let us again consider an oxide in which the relevant oxygen defects are oxygen vacancies ( $V_\delta$ ) and also allow for a lower-valent doping. The ionic defect may be compensated by an immobile counter-defect which can be native, such as  $V_{\text{Sr}}''$  in  $\text{SrTiO}_3$ ,<sup>7,8</sup> or an acceptor dopant with a fixed valence such as  $\text{Y}^{3+}$  in  $\text{ZrO}_2$ .<sup>2,9</sup> The oxygen vacancies can also be compensated by a redox-active acceptor dopant such as  $\text{Fe}^{3+}$  in  $\text{SrTiO}_3$ . Further situations are encountered if the oxygen vacancies are compensated by conduction electrons, as is formally the case in these oxides at extremely low  $P_{O_2}$ , or if the electronic defects (in this case hole dominance) are in the majority and compensated by the (lower-valent) dopant, be they redox-inactive or redox-active. Thus, in accordance with the relevant chemical diffusion scheme in Fig. 1 in which the mass transport is established by  $V_\delta$  as the ionic and  $h^\bullet$  as electronic entities, the latter being subject to trapping by the immobile  $\text{Fe}^{3+}$  impurities, we have distinguished between five different defect chemical situations.

For our purpose this can be narrowed down to two qualitatively different situations. First to the case (case I) in which the redox-active impurity is not in the majority, as generally fulfilled for  $\text{Y}_2\text{O}_3$ -doped  $\text{ZrO}_2$  (YSZ), as long as we can assume  $[Y_{\text{Zr}}']$  to be a constant. In this case,  $[V_\delta]$  is given by  $[Y_{\text{Zr}}']/2$ . Pure  $\text{SrTiO}_3$  also belongs to this case. Here,  $V_\delta$  is compensated by the Sr vacancies formed according to the SrO Schottky reaction at very high temperatures. If  $[V_{\text{Sr}}'']$  is frozen-in at the temperatures under consideration we obtain, as in the YSZ case,

$$[V_\delta] = \text{constant} \quad (9)$$

and

$$[h^\bullet] \propto \text{constant} \times K_O^{1/2} P_{O_2}^{1/4} \quad (10)$$

both being independent of any redox-active impurity content,  $m_i$ . In eqn. (10),  $K_O$  is the oxygen incorporation reaction corresponding to the occupation of one oxygen vacancy and release of two holes:

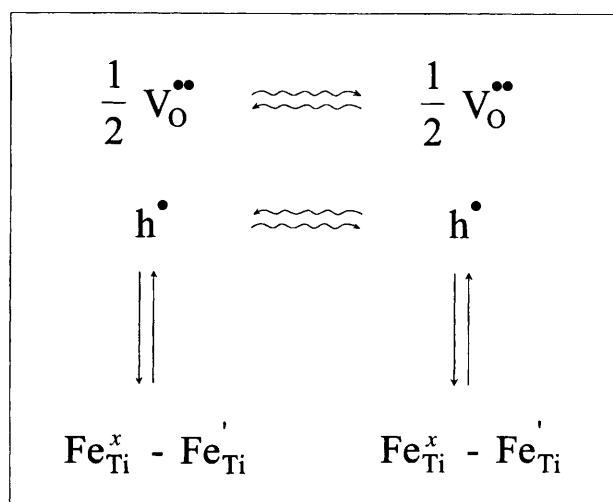
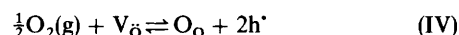


**Fig. 1** Schematic representation of the buffered chemical diffusion relevant to our examples. The horizontal axis represents the spatial coordinate. The counter-flux of  $V_\delta$  and  $2 h^\bullet$  constitutes the mass transport of oxygen. The holes are, in addition, subject to an internal trapping reaction with the dopant ions.

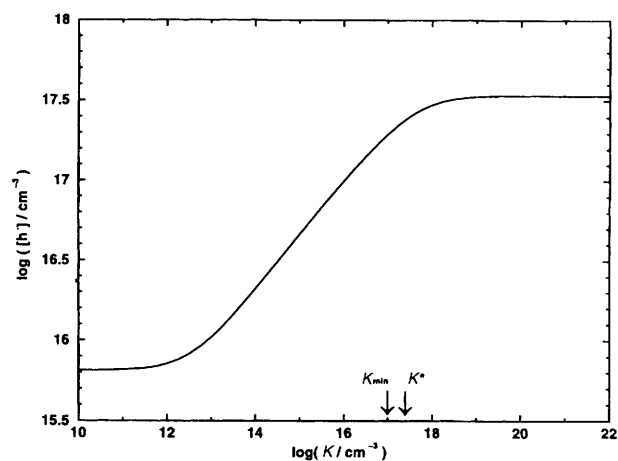


**Fig. 2** Calculation of the  $h'$  concentration as a function of the equilibration constant,  $K$ , for  $T = 900$  K and  $P_{O_2} = 10^5$  Pa ( $m_{Fe} = 10^{19}$  cm $^{-3}$ , Sr vacancy concentration =  $10^{16}$  cm $^{-3}$ ). The other simulation parameters are quoted in the Appendix.

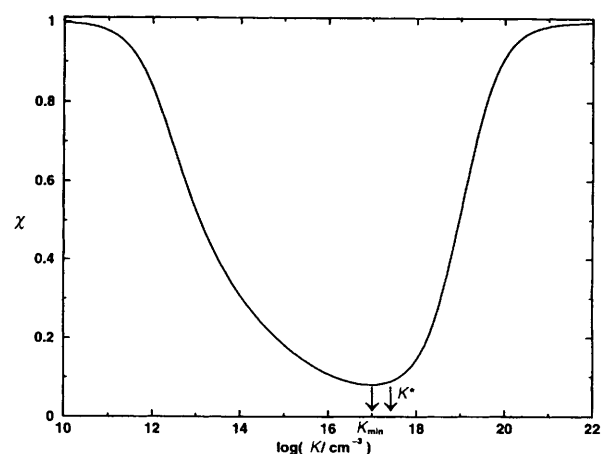


**Fig. 3** Calculation of the trapping factor,  $\chi$ , as a function of the equilibration constant,  $K$ , for  $T = 900$  K and  $P_{O_2} = 10^5$  Pa ( $m_{Fe} = 10^{19}$  cm $^{-3}$ , Sr vacancy concentration =  $10^{16}$  cm $^{-3}$ ). The minimum of the trapping factor is found at  $K = 10^{17}$  cm $^{-3}$ .

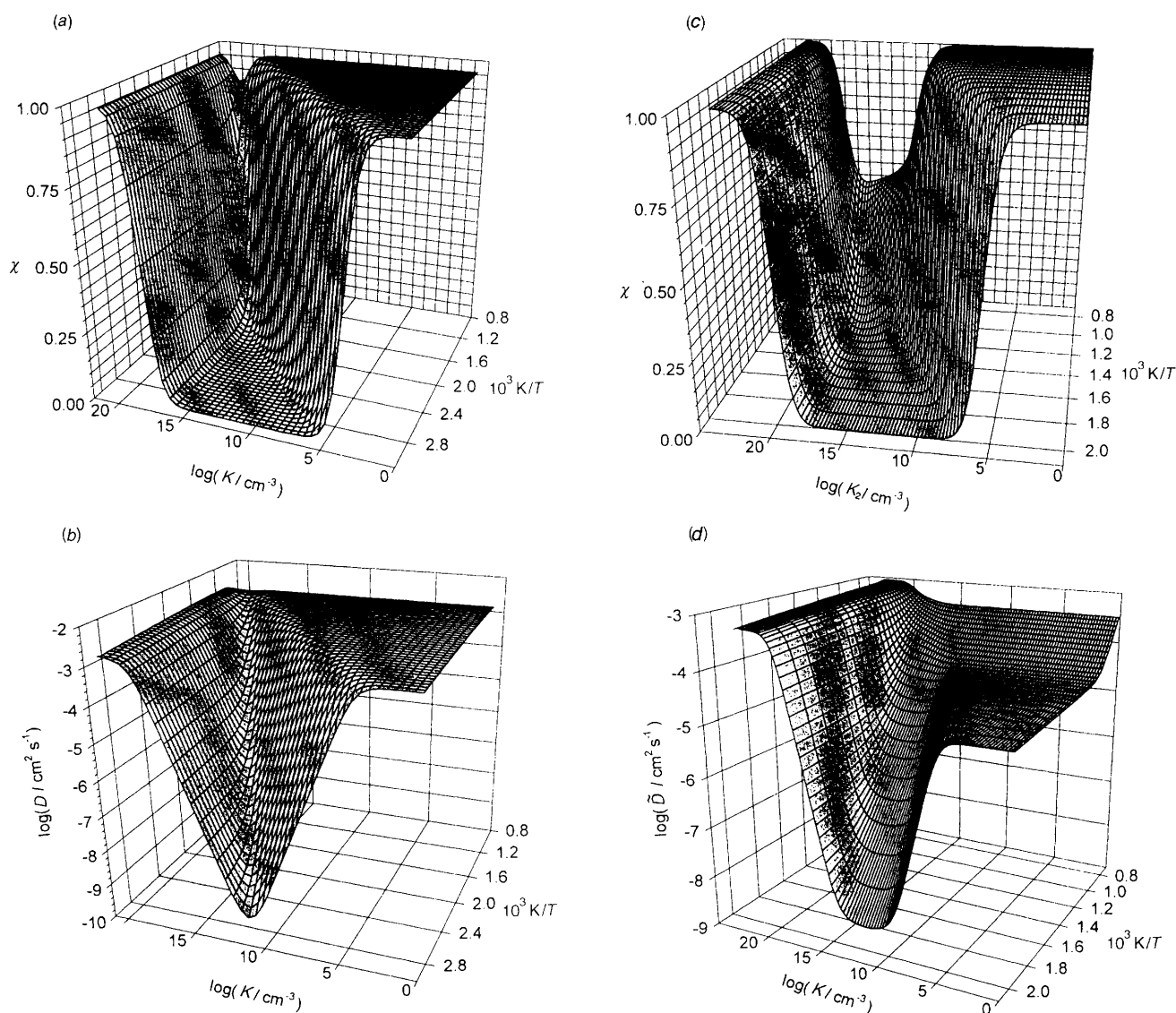


**Fig. 4** The trapping factor,  $\chi$ , and the diffusion coefficient,  $\tilde{D}$ , plotted as a function of the reciprocal temperature,  $10^3$  K/T, and the equilibration constant,  $K$ , for case I:  $[V_{Sr}] = 1000 m_{Fe}$  (a), (b) and case II:  $[V_{Sr}] = 0.001 m_{Fe}$  (c), (d). The oxygen partial pressure was set to  $10^5$  Pa. The other numerical parameters are stated in the Appendix.



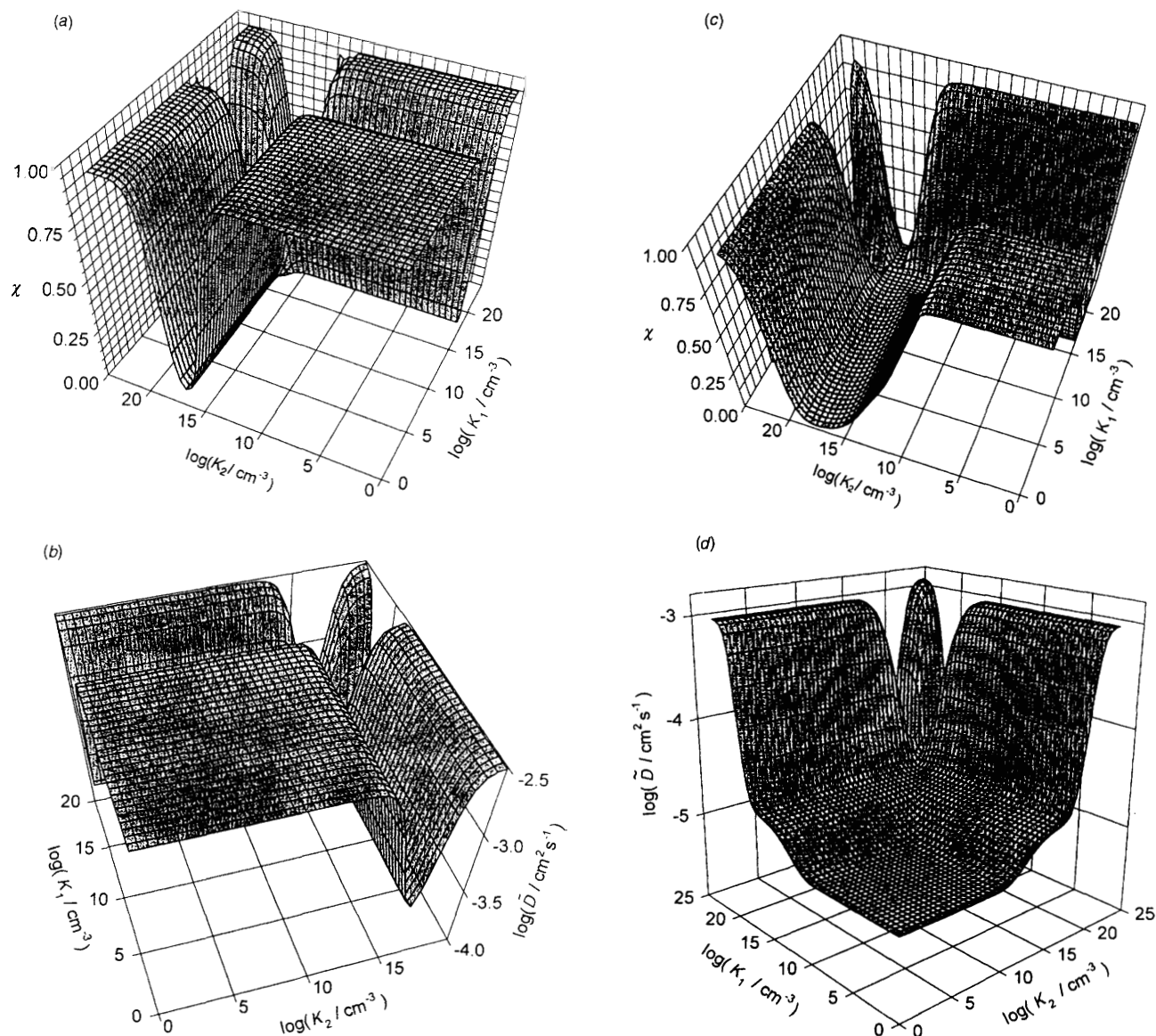


**Fig. 5** The trapping factor,  $\chi$ , and the diffusion coefficient,  $\tilde{D}$ , in the presence of two dopants plotted with equilibrium constants  $K_1$  and  $K_2$  for case I:  $[V_{Sr}^{''}] = 1000m_1 = 1000m_2$  (a), (b) and case II:  $[V_{Sr}^{''}] = 0.001m_1 = 0.001m_2$  (c), (d). The temperature was set to 900 K,  $P_{O_2} = 10^5$  Pa. The other numerical parameters are stated in the Appendix ( $m_1 = m_2 = m_K$ ).

If we consider the very high temperatures at which the Schottky process is in equilibrium, such that  $[V_{\text{O}}] = [V_{\text{Sr}}^{''}] \propto K_s(T)^{1/2}$ , the constant in eqn. (10) has to be replaced by the  $T$ -dependent  $K_s^{1/2}$  value. The situation at extremely low oxygen partial pressures where  $2[V_{\text{O}}] = [e']$  is very similar to this case. There, a  $P_{O_2}^{-1/6}$  power law results for the electron concentration (now  $[e']$  instead of  $[h']$ ). Under all circumstances, simple power law dependences are obtained and  $[h']$ ,  $[V_{\text{O}}]$  and  $[e']$  do not depend on  $m_i$ . As a consequence, the impact of the redox-active impurities on  $\tilde{D}$  is reflected by the effect on  $\chi_i$ .

The second key situation (case II) is encountered if the redox-active impurities appear in the electroneutrality equation as majority carriers, as in  $\text{SrTiO}_3$  if the redox-active impurity content is higher than the Sr vacancy content. Then the redox equilibrium affects  $[h']$  directly, and the impact of the  $K_i$  on  $\chi$  and  $\tilde{D}$  differs.

Let us first investigate  $\chi \equiv \chi_{h'}$  and restrict to one type of redox-active impurity  $m_i = m$  and  $K_i = K$ . Since

$$\chi = \frac{1}{1 + \frac{mK}{(K + [h'])^2}} \quad (11)$$

the total change in  $\chi$  due to a change in the nature of the redox-active impurity is given by

$$\frac{d\chi\{K, [h'](K)\}}{dK} = \left(\frac{\partial\chi}{\partial K}\right)_{[h']} + \left(\frac{\partial\chi}{\partial[h']}\right)_K \frac{d[h']}{dK} \quad (12)$$

Note that  $m$  and  $P_{O_2}$  are kept constant.

In the first case of consideration (case I), the second term vanishes due to  $d[h']/dK = 0$ , such that

$$\frac{d\chi}{dK} = \frac{\partial\chi}{\partial K} = \frac{(K^2 - [h']^2)m}{\{(K + [h'])^2 + mK\}^2} \quad (13)$$

i.e. we obtain a minimum ( $K_{\min}$ ) exactly for that equilibrium constant ( $K^*$ ) for which  $K$  and  $[h']$  are equal, i.e.  $K_{\min} = K^*$ . Each dopant results in an individual equilibrium hole concentration ( $m$ ,  $P_{O_2}$  being constant). This kind of doping, providing an equilibrium hole concentration which coincides with  $K$ , exhibits the most pronounced effect in diminishing  $\chi$  and thus  $\tilde{D}$ .

In view of eqn. (7) and (12), this is exactly fulfilled if  $[\text{ox}] (\equiv [A^{n'}])$  and  $[\text{red}] (\equiv [A^{(n+1)}])$  coincide. In this way it is justified to speak of a dynamic buffer effect on the

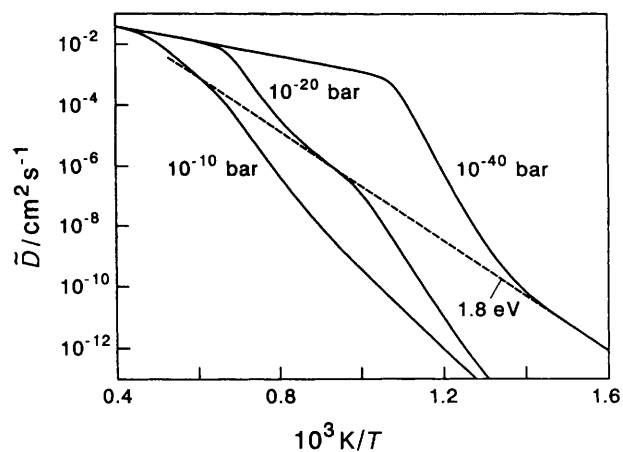


**Fig. 6** Model calculation of the oxygen diffusion coefficient in YSZ, as a function of  $T$  for different  $P_{O_2}$  with a Ti dopant concentration of  $m_{Ti} = 10^{19} \text{ cm}^{-3}$  and a Ce dopant concentration of  $m_{Ce} = 2 \times 10^{18} \text{ cm}^{-3}$ , taken from ref. 6.

diffusion<sup>10</sup> as  $x_h = \delta[h^*]/\delta[h]^*$  expresses the increase of the free hole concentrations when the total concentration is increased, *i.e.* a buffer capacity. Note again that this buffer capacity does not enter the equilibrium concentrations.

It is also worth investigating the limits of  $\chi$  for the case of the prevalence of a given valence state. If  $K$  becomes extremely large, *i.e.* if  $m \approx [\text{red}] \gg [\text{ox}]$ ,  $\chi$  tends to 1, independent of the behaviour of  $[h^*]$ . For vanishing  $K$ , *i.e.*  $m \approx [\text{ox}] \gg [\text{red}]$ , the same limit (*viz.* 1), results, provided that  $[h^*]$  does not simultaneously vanish (which is fulfilled for the case considered here). The electroneutrality conditions are in this case  $[V_{Sr}'] = [V_{O}']$  for  $\text{SrTiO}_3$  and  $[Y_{Zr}'] = 2[V_{O}']$  for YSZ.

Let us investigate the limits and the minimum for the second case (case II) in which the redox-active impurity is in the majority. We choose the case that  $2[V_{O}'] = [\text{Fe}_{Ti}']$ . The limit for  $K \rightarrow \infty$  is still 1. If  $K \rightarrow 0$  only the neutral  $\text{Fe}_{Ti}^x$  impurity defect is present. In this case  $[V_{O}']$  is limited by the  $V_{Sr}'$  content and  $\chi \rightarrow 1$  as above.

If we assume the absence of Schottky defects,  $[\text{Fe}_{Ti}'] = [h^*]$

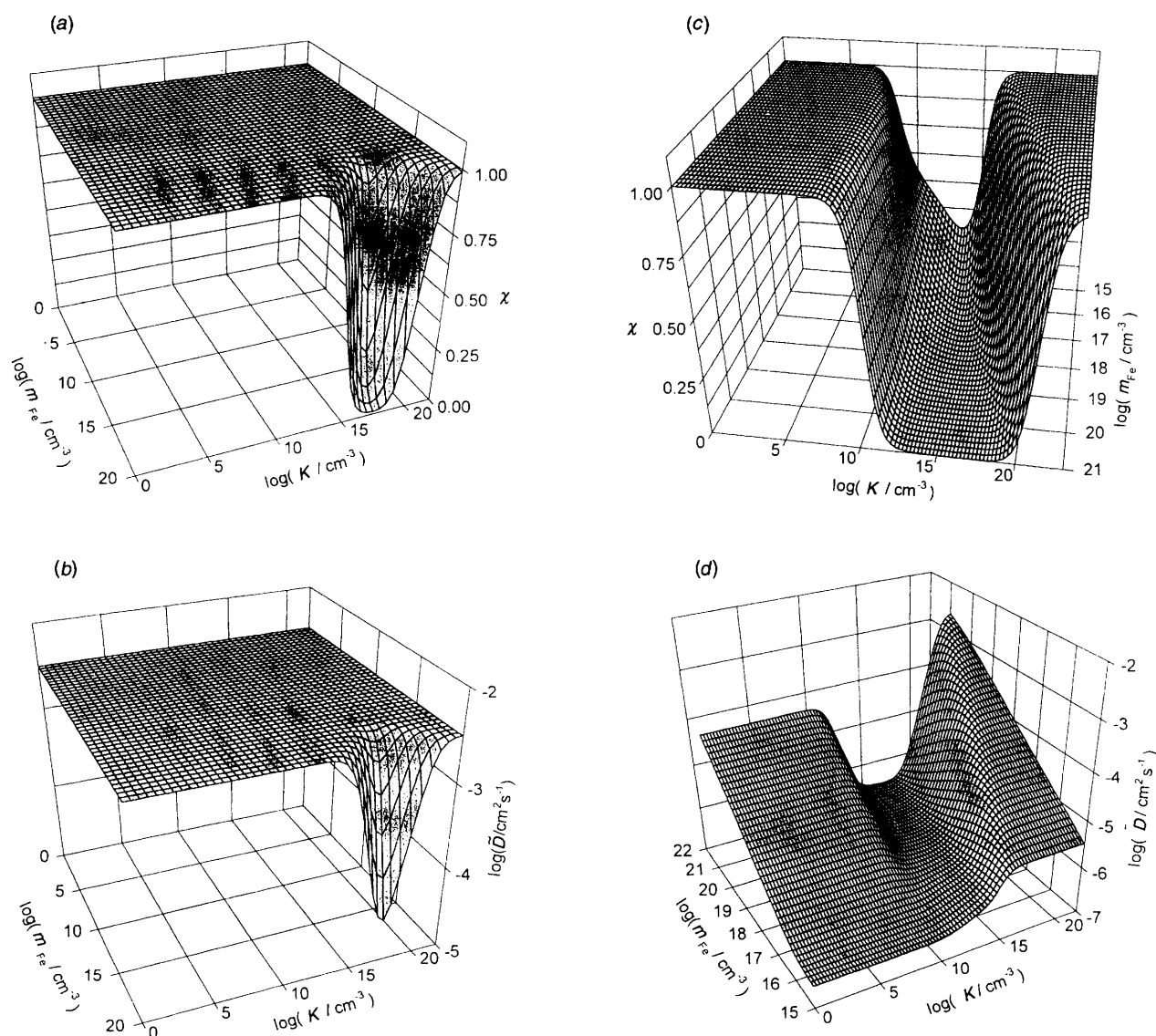


**Fig. 7** The trapping factor,  $\chi$ , and the diffusion coefficient,  $\bar{D}$  plotted as a function of the Fe dopant content and the equilibration constant,  $K$ , for case I:  $[V_{Sr}']$  has been fixed at the (artificial) value of  $10^{22} \text{ cm}^{-3}$  (a), (b); and for case II:  $[V_{Sr}'] = 10^{-12} \text{ cm}^{-3}$  (c), (d). The temperature was set to 900 K,  $P_{O_2} = 10^5 \text{ Pa}$ . The other numerical parameters are stated in the Appendix.



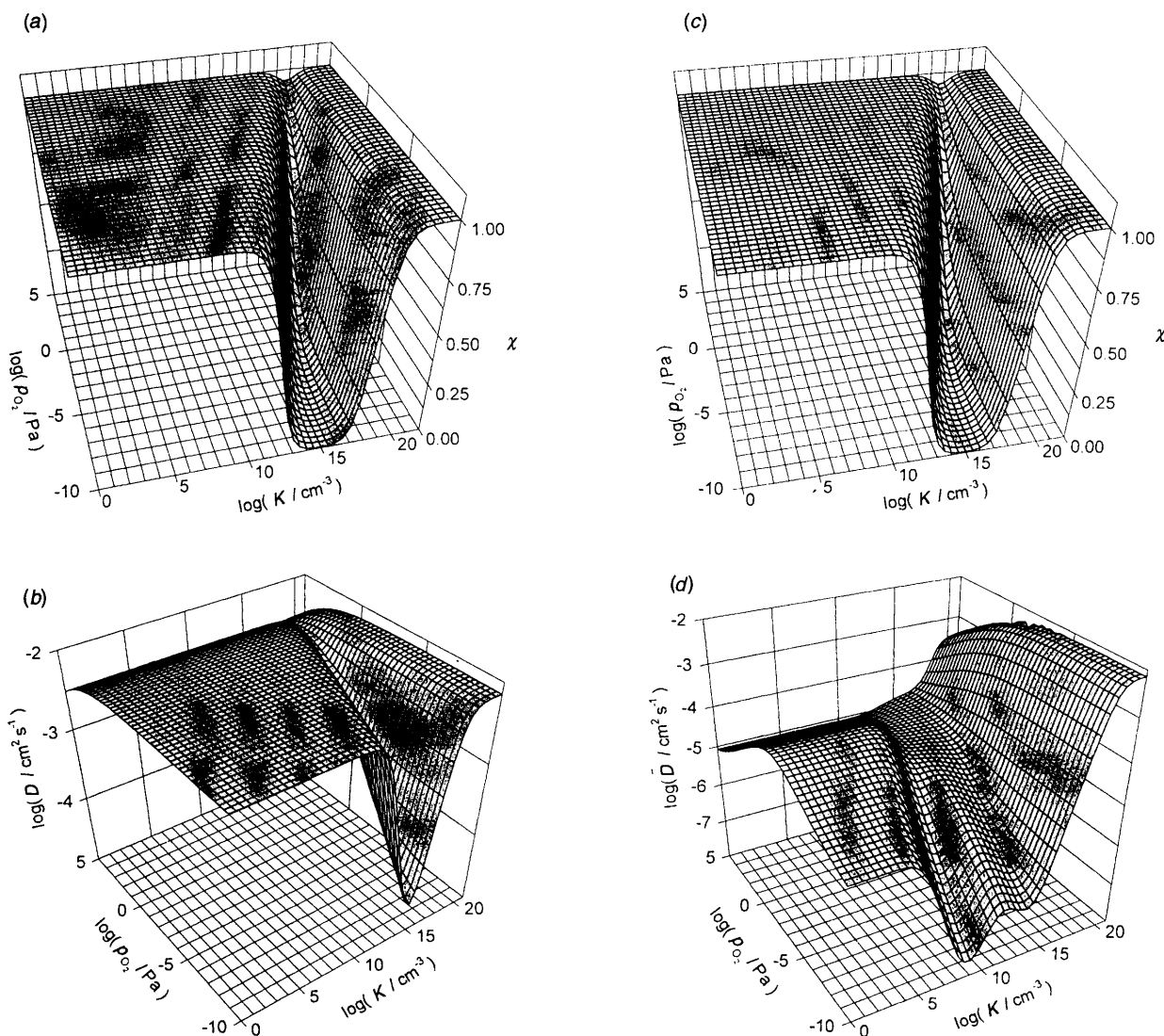


**Fig. 8** The trapping factor,  $\chi$ , and the diffusion coefficient,  $\tilde{D}$ , plotted as a function of the oxygen partial pressure,  $P_{O_2}$ , and the equilibration constant,  $K$ , for case I:  $[V_{Sr}] = 1000m_{Fe}$  (a), (b) and case II:  $[V_{Sr}] = 0.001m_{Fe}$  (c), (d). The temperature was set to 900 K. The other numerical parameters are stated in the Appendix.

results; both terms, however, approach zero. Then  $\chi$  tends† to  $(1 + [Fe_{Ti}^x]K/[Fe_{Ti}'] [h']^{-1})^{-1} = 1/2$ , which is, however, an unrealistic situation. More important, as far as the second case is concerned, is the fact that the minimum is no longer at  $K = K^*$ , i.e. not at  $[ox] = [red]$ , since  $d[h']/dK \neq 0$ .

As long as, however,  $m \approx [Fe_{Ti}'] \approx 2[V_{O}]$ , i.e. for not too low  $K$  values, the differential quotient will not be far from that value ( $[h']$  depends on  $m$  but not very much on  $K$  and the result is of the form of eqn. (10)). Fig. 2 and 3 indicate that the minimum,  $K_{min}$ , is still roughly at  $K^*$ , i.e. at  $[h'] \approx K$ ,  $d[h']/dK$  being small. The data set (see Fig. 2) gives more exactly that  $K_{min} < K^*$  implying  $d[h']/dK|_{K^*} > 0$  since  $(\partial\chi/\partial[h'])_K = 2mK(K + [h'])/(mK + (K + [h'])^2)^2$  is always positive. Fig. 4–8 show various situations with one or two dopants (exhibiting significantly different ionisation constants) calculated for  $SrTiO_3$  for the two cases considered above:  $[V_{Sr}] \gg m$  in case I and  $m \gg [V_{Sr}] \neq 0$  in case II. In all cases we regard  $m$  and  $[V_{Sr}]$  as constants with respect to  $T$  and

$P_{O_2}$ . The data set used<sup>8</sup> is given in the Appendix. Note that the dependence on  $\log K$ , which is presented in the figures, chiefly reflects the dependence on the corresponding energy level.

It can be seen immediately from Fig. 4 that, as expected, the  $\tilde{D}$  and  $\chi$  dependences look different if  $m \gg [V_{Sr}]$  [case II, see above, see Fig. 4(c), (d)] but qualitatively similar if  $m \ll [V_{Sr}]$  [case I, Fig. 4(a), (b)]. As discussed above, the reason is that  $c_{V_O}$  and  $c_h$  do and do not depend on  $K$  in cases II and I, respectively. Note how sharply the kinetic parameters can be tuned. The pronounced minima in the figures are particularly evident. It is obvious that  $K_{min}$  is close to  $K^*$  which represents the mass action constant generating a ratio of  $[ox]$  and  $[red]$  of unity. Also, limits of 1 for  $\chi$  are obtained [Fig. 4(a), (c)], as already given in Fig. 2. The structure becomes more difficult to elucidate if we consider two redox-active dopants with significantly different ionisation parameters (Fig. 5). Fig. 6 gives the temperature dependence of  $\tilde{D}$  in YSZ as computed in ref. 6 for two different traps revealing themselves as two distinct knees.

Returning to the situation with one dopant, Fig. 7 demonstrates the influence of its total concentration. The sensitivity of  $\chi$  on  $m$  in case I is worth noting, while in case II  $\chi$  depends on  $m$  only weakly ( $[h']$  increases with  $m$ ). Fig. 8 indicates that a remarkable  $P_{O_2}$  dependence occurs in the region of substantial trapping, as is clear from eqn. (11); in addition, a signifi-

$$\begin{aligned} \dagger \frac{mK}{(K + [h'])^2} &= \frac{mK}{\left(K + \frac{K(m - [Fe'])}{[Fe']}\right)^2} \rightarrow \frac{m}{K} \frac{1}{\left(1 + \frac{m}{[Fe']}\right)^2} \\ &\approx \frac{m}{K} \frac{[Fe']^2}{m^2} \approx \frac{[Fe']^2}{Km} \approx \frac{[Fe']^2}{K[Fe']} \end{aligned}$$

cant  $P_{O_2}$  dependence results in Fig. 8(d) over the whole parameter range, since in that case ( $m_{Fe} \gg [V_{Sr}']$ ) the ionic and electronic point defect densities themselves depend sensitively on  $P_{O_2}$ , in particular  $\sigma_{V\delta}/\sigma$ , and thus the ratio  $\tilde{D}/\chi$  according to eqn. (3), even leading to an additional sharp minimum at  $K_2 \ll K^*$ .

#### 4. Implications for diffusion experiments and applications

The relevance of such trapping effects for chemical diffusion in mixed or ionic conductors has already been stressed in previous papers.<sup>3,5,2,10,11</sup> These considerations allow for a quantitative description of the experimental diffusion data obtained by different methods in SrTiO<sub>3</sub> and YSZ. In the first case, a very accurate quantitative description of  $\tilde{D}$  was possible as a function of temperature, dopant content and oxygen partial pressure, as outlined in ref. 11 and 12. YSZ<sup>6,10,13</sup> is the simplest and, qualitatively speaking, most striking case in this context, and shall be briefly taken up again.

If we first concentrate on high  $P_{O_2}$ , redox changes of  $[Y'_{Zr}]$  and  $[V_{\delta}]$  may be neglected: Any redox-active impurity is negligible in the electroneutrality equation (in absolute terms). Since all equilibrium defect concentrations derive from the oxygen incorporation reaction, the electroneutrality equation and possible interaction reactions, the results for the equilibrium concentrations of  $[V_{\delta}]$  and  $[h']$  will not depend on redox-active traces at all. Ignoring such redox-active impurities also for  $\tilde{D}$  would result in  $\tilde{D} = D_{h'}$ , since both  $c_{V\delta}$  and  $\sigma_{V\delta}$  exceed  $c_{h'}$  and  $\sigma_{h'}$  by far [see eqn. (1)]. If this were true, as has been assumed in the literature, the  $\tilde{D}$  values would not depend on redox-active impurities, not on  $P_{O_2}$  and only weakly on  $T$ . However: (i) it is found that the numerical values in the literature scatter by orders of magnitude. (ii) We found a strong dependence on the amount of deliberately added transition-metal impurities ( $m \ll [Y'_{Zr}]$ ). (iii)  $\tilde{D}$  also depends strongly on  $T$  and somewhat on  $P_{O_2}$ . The effects of such impurities can be analysed by considering the exact solution of eqn. (3), which for YSZ reduces to  $\tilde{D} = D_{h'}\chi_{h'}$ , these dependences result from  $\chi = \chi(T, P_{O_2}, [Y'_{Zr}], m)$ . The diverging literature results can be explained by the unexpected presence of impurities.<sup>13</sup> At low  $P_{O_2}$  self-trapping of  $e^-$  by  $V_{\delta}$  or  $Y'_{Zr}$  may also be possible. However, it is more likely that Ti impurities are dominant in this respect, at least in the examples analysed in ref. 6. (Of course, experimental difficulties may also have contributed to the scatter.<sup>14</sup>) It is worth mentioning again that the impact of the redox-active centres on  $\tilde{D}$  results from the differential change in the electroneutrality equation, which is important for  $\chi$ . Even though these impurities are negligible with respect to  $[Y'_{Zr}]$ , it is not at all true for the changes.

It is obvious from the preceding section that those impurities are most active, the corresponding ionisation constants of which allow for a comparable ratio of the reduced to the oxidised forms. This is evidently best fulfilled if the energy levels are not too close to the band edges.

In other words, by knowing the relevant parameters we can design  $\tilde{D}$  values by appropriate doping. To give an example, in the boundary conductivity sensor drift effects occur if the  $\tilde{D}$  values are significant. Doping the oxide with appropriate impurities should give rise to significant improvements in this respect. Of course, competing influences on the performance, e.g. via the sensitivity, have to be considered simultaneously.<sup>15</sup>

#### Appendix

Defect-chemical parameters used for SrTiO<sub>3</sub>.<sup>12</sup>

$$K_O(T) = K_O^\circ \exp\left(-\frac{E_O}{k_b T}\right) \left( = \frac{[h']^2}{[V_{\delta}]P_{O_2}^{1/2}} \right)$$

$$K_B(T) = K_B^\circ \exp\left(-\frac{E_B - \beta_B T}{k_b T}\right) (= [h'] [e'])$$

$$K(T) = K^\circ \exp\left(-\frac{E - \beta T}{k_b T}\right) \left( = \frac{[Fe'_{Ti}][h']}{[Fe^{x}_{Ti}]} \right)$$

$$K_O^\circ = 1.02 \times 10^{23} \text{ Pa}^{-1/2} \text{ cm}^{-3}$$

$$K_B^\circ = 7.67 \times 10^{42} \text{ cm}^{-6}$$

$$K^\circ = 2.77 \times 10^{21} \text{ cm}^{-3}$$

$$E_O = 1.63 \text{ eV}$$

$$E_B = 3.3 \text{ eV}$$

$$E = 1.18 \text{ eV}$$

$$\beta_B = 6.0 \times 10^{-4} \text{ eV K}^{-1}$$

$$\beta = 3.7 \times 10^{-4} \text{ eV K}^{-1}$$

$$u_p = 8.9 \times 10^5 (T/K)^{-2.36} \text{ cm}^2 \text{ V}^{-1} \text{ s}^{-1} \text{ (mobility of } h')$$

$$u_n = 4.5 \times 10^5 (T/K)^{-2.2} \text{ cm}^2 \text{ V}^{-1} \text{ s}^{-1} \text{ (mobility of } e')$$

$$u_v = 1.0 \times 10^4 \text{ cm}^2 \text{ V}^{-1} \text{ s}^{-1} (T/K)^{-1} \exp\left(-\frac{0.86 \text{ eV}}{k_b T}\right) \\ \text{(mobility of } V_{\delta})$$

$$k_b = 8.617 \times 10^{-5} \text{ eV K}^{-1} \text{ (Boltzmann constant)}$$

if not stated otherwise:

$$m = m_{Fe} = 10^{19} \text{ cm}^{-3}$$

$$T = 900 \text{ K}$$

$$P_{O_2} = 10^5 \text{ Pa}$$

#### References

- 1 C. Wagner, in *Progress in Solid State Chemistry*, ed. H. Reiss, Pergamon Press, Oxford, 1971, vol. 6; H. Schmalzried, *Solid State Reactions*, Verlag Chemie, Weinheim, 1981.
- 2 L. Heyne, *Solid Electrolytes*, ed. S. Geller, Springer Verlag, Berlin, 1977.
- 3 J. Maier and G. Schwitzgebel, *Phys. Stat. Sol. (b)*, 1982, **113**, 535; J. Maier, *J. Am. Ceram. Soc.*, 1993, **76**, 1212.
- 4 J. Maier, *Solid State Ionics*, 1992, **57**, 71.
- 5 J. Maier, *J. Am. Ceram. Soc.*, 1993, **76**, 1223.
- 6 R. I. Merino, N. Nicoloso and J. Maier, *Proc. Br. Ceram. Soc. Conf. on Ceram. Oxygen Ion Cond. and Their Techn. Appl.*, to be published.
- 7 J. Daniels, K.-H. Härdtl, D. Hennings and R. Wernicke, *Philips Res. Reps.*, 1976, **31**, 487; N. H. Chan, R. K. Sharma and D. M. Smyth, *J. Electrochem. Soc.*, 1981, **128**, 1762; R. Waser, *J. Am. Ceram. Soc.*, 1991, **74**, 1934; G. M. Choi and H. L. Tuller, *J. Am. Ceram. Soc.*, 1988, **71**, 201.
- 8 I. Denk, W. Münch and J. Maier, *J. Am. Ceram. Soc.*, 1995, **78**, 3265.
- 9 L. Heyne and N. M. Beckmans, *Proc. Br. Ceram. Soc.*, 1970, **19**, 229; J. H. Park and R. N. Blumenthal, *J. Electrochem. Soc.*, 1989, **136**, 2867.
- 10 J. Maier, in *Ionic and Mixed Conducting Ceramics*, ed. T. A. Ramanarayanan, W. L. Worrell and H. L. Tuller, The Electrochem. Soc., Pennington, 1994, vol. 94-12, p. 542.
- 11 T. Bieger, J. Maier and R. Waser, *Ber. Bunsen-Ges. Phys. Chem.*, 1993, **97**, 1098.
- 12 I. Denk, F. Noll and J. Maier, *J. Am. Ceram. Soc.*, submitted.
- 13 T. Bieger, H. Yugami, N. Nicoloso, J. Maier and R. Waser, *Solid State Ionics*, 1994, **72**, 41.
- 14 J. Maier, *Solid State Phenom.*, 1994, **39–40**, 35.
- 15 J. Maier, *Solid State Ionics*, 1989, **32/33**, 727.

Paper 6/00951D; Received 9th February, 1996